Fuzzy Systems and Data Mining IX
A.J. Tallón-Ballesteros and R. Beltrán-Barba (Eds.)

doi:10.3233/FAIA231041

Research on Dynamic Multi-Layer Block Network Evolution Based on Bayesian Inference

Yuping Tang[a] , Yingzi Fu[b, 1] and Yeqing Ding[b]
[a] College of Science, Kunming University of Science and Technology, China
[b] Applied Statistics Research Center, Kunming University of Science and Technology, China

Abstract. Dynamic multi-layer network analysis is the frontier direction of network science and a prominent challenge in the field of complex network systems. In this paper, a covariate-assisted dynamic multi-layer network community detection method is proposed, which effectively combines the dependence within each network, across time and between different layers. The latent Gaussian process is used to model the edge probability between participants, and a flexible time series analysis is obtained. An extended model based on community is proposed to reduce the computational burden. In terms of parameter estimation, this paper uses the Bayesian method to conduct posterior inference on model parameters. Finally, a set of real business relationship network data is used for experiments, and the results show that the dynamic multilayer block network model has lower estimation time cost and better prediction performance, and the chunking structure of its model is more capable of revealing meaningful community structures, which makes it suitable for dealing with more complex dynamic networks.

Keywords. Dynamic multi-layer blocks; edge covariates; gaussian process; latent space

1. Introduction

Social network research focuses on the analysis of the dependencies between people or other social units, that is, the dependencies caused by the ties that bind them together [1-2]. Nowadays, there is a growing interest in the dynamic interdependencies of networks with other structures. However, these dynamic interactions[3] across time usually occur in multilayer connections, and thus multilayer networks are jointly modeled to fully understand the evolution of the complex network structure under study over time.

Data on social interaction processes are rapidly becoming highly multidimensional, and the availability of multidimensional networks in World Wide Web architectures[4], telecommunication infrastructures[5], and so on continues to increase. A growing number of research directions indicate the need for appropriate approaches to address the

[1] Corresponding Author, Yingzi Fu, Applied Statistics Research Center, Kunming University of Science and Technology, Kunming Yunnan 650500, China; E-mail: 2213971143@qq.com.

complexity associated with network problems, and network modularity analysis[6], network resilience analysis[7], etc. are examples of these new directions.

In recent years, statistical models for multi-layer networks have increased. The latent space model first proposed by Hoff et al.[8] is a classic model because it can flexibly capture common network features, such as node degree heterogeneity, transitivity, homogeneity, etc. Gollini and Murphy[9] and DAngelo et al.[10] proposed a latent space model for multi-layer networks. It is assumed that the latent representation of each node is the same on all layers, and the changes between networks are captured by layer-specific parameters that control the overall network characteristics. Durante and Dunson[11-12] introduced continuous-time dynamics by considering the Gaussian process of potential coordinate evolution over time, and then they extended the model in 2016[13]. Durante et al.[14] proposed a dynamic multi-layer network model, which considers a shared latent space to capture the global structure and a K-layer specific latent space that characterizes the special structure of each layer. On this basis, Carmona et al.[15] proposed a general network model for longitudinal data of multi-layer networks with directed and weighted edges in 2019 to analyze the dynamic multi-layer network structure changes over time more comprehensively. Dealing with large networks is often computationally difficult, however; Yildirimoglu and Kim[16] used modularity-based community monitoring to find demand patterns in a multilayered urban environment for demand analysis at different spatial resolutions. Yap et al.[17] used graph-based community detection to determine which wiring harnesses within the selected hubs to synchronize in order to be applicable to the context of the current public transportation. and Tian et al.[18] significantly reduced the computational cost of the large-scale rebalancing problem by partitioning the shared bicycle network. In 2022, Hector et al.[19] proposed a new probabilistic latent network model to predict multi-layer dynamic graphs that are increasingly common in transportation.

Inspired by the above work, the contributions of this paper's work are as follows. First, this paper proposes a covariate-assisted community monitoring approach for dynamic multilayer networks that effectively combines dependencies within each network, across time, and between different layers, while maintaining flexibility. Second, the computational burden is reduced by jointly considering both the temporal and spatial dimensions of the network to provide an in-depth demonstration of the evolution of the dynamic multilayer network structure over time. Finally, a set of real business relationship network data is used as an example to validate the method, and the experimental results prove that it has lower estimation time cost and better prediction performance, and is suitable for dealing with more complex dynamic networks.

2. Dynamic multi-layer block network model

The dynamic multilayer graph has each layer of graph that evolves over time, and can be represented by $V \times V$ adjacency matrix $Y^k(t)$, each matrix has a binary element $Y_{ij}^k(t) = Y_{ji}^k(t) \in \{0,1\}$, which measures whether there is a connection between nodes i and j. If there is a connection between participants i and j at time $t = t_1, ..., t_n$ on the $k = 1, ..., K$ -th layer, then $Y_{ij}^k(t) = 1$.

To strengthen the community structure, each node in the network is assumed to belong to a random block[20] or cluster such that the probability of the existence of an edge between any two nodes in the network depends on which block or cluster $b \in \{1,...,B\}$ they belong to. Thus the estimation will be performed on $B(B+1)/2$ blocks rather than on $N(N-1)/2$ nodes, where $B \ll N$, significantly reduces the computational cost. The prior probability is set to $p(z_i = b) = \eta_b$, where z is the vector assigned to the block, indicating that each participant i belongs to which block, and $\eta \sim Dirichlet(\alpha_1,...,\alpha_B)$. The model is extended by considering the inclusion of covariates, specifically the joint modeling of inter-block and intra-block connection probabilities as follows.

$$z_i \sim Categorical(\eta_1,...,\eta_B) \tag{1}$$

$$Y_{ij}^k(t) \big| (z_i = p, z_j = q) \sim Bernoulli(\pi_{pq}^k(t)) \tag{2}$$

$$\psi_{pq}^k(t) = Logit(\pi_{pq}^k(t)) = \begin{cases} \mu(t) + \sum_{r=1}^{R} \bar{x}_{pr}(t)\bar{x}_{qr}(t) + \sum_{h=1}^{H} x_{ph}^k(t)x_{qh}^k(t) + \beta_m(t)' g_{ij}^k(t), & p \neq q \\ \mu_p^k(t) + \sum_{r=1}^{R} \bar{x}_{pr}(t) & , \text{ p=q} \end{cases} \tag{3}$$

3. Bayesian posterior inference

The full data likelihood of the model presented in this paper is:

$$p(Y_{ij}^k(t) | \psi_{pq}^k(t)) = \prod_{t=1}^{T}\prod_{k=1}^{K}\prod_{i=2}^{V}\prod_{j=1}^{i-1} \frac{\exp(\psi_{z_i z_j}^k(t))^{Y_{ij}^k(t)}}{1+\exp(\psi_{z_i z_j}^k(t))} = \prod_{t=1}^{T}\prod_{k=1}^{K}\prod_{p=1}^{B}\prod_{q=1}^{p} \frac{\exp(\psi_{pq}^k(t))^{y_{pq}^k(t)}}{\left[1+\exp(\psi_{pq}^k(t))\right]^{n_{pq}^k(t)}} \tag{4}$$

Where $\psi_{pq}^k(t) = Logit(\pi_{pq}^k(t))$, $n_{pq}^k(t)$ and $y_{pq}^k(t)$ denote the number of possible edges and actual edges in $Y_{ij}^k(t)$ between blocks p and q, respectively.

3.1. Gaussian Process Prior for Time - Varying Latent Coordinates

Inspired by the dynamic modeling of a single network, the Gaussian process prior considering the potential coordinates of participants is defined as follows :

$$\mu(t) \sim GP(0, c_\mu), \quad \mathrm{c}_\mu(t_i, t_j) = \exp\left\{-k_\mu (t_i - t_j)^2\right\}, \quad \mathrm{k}_\mu > 0 \tag{5}$$

$$\bar{x}_{ir}(t) \sim GP(0, \tau_r^{-1} c_{\bar{x}}), \quad c_{\bar{x}}(t_i, t_j) = \exp\left\{-k_{\bar{x}} (t_i - t_j)^2\right\}, \quad k_{\bar{x}} > 0 \tag{6}$$

$$x_{ih}^{k}(t) \sim GP\left(0, \tau_h^{k-1} c_x\right), \quad c_x\left(t_i, t_j\right) = \exp\left\{-k_x\left(t_i - t_j\right)^2\right\}, \quad k_x > 0 \tag{7}$$

independently for $i = 1,...,V$, r=1,...,R, h $= 1,...,H$, $k = 1,...,K$, $c_{\bar{x}}\left(t_i, t_j\right)$ and $c_x\left(t_i, t_j\right)$ in Equations (6) and (7) represent the square exponential correlation function of the Gaussian process with shared and layer-specific potential coordinates, respectively. $\tau_1^{-1},...,\tau_R^{-1}$ and $\tau_1^{k-1},...,\tau_H^{k-1}$ are the positive shrinkage parameters of the control potential coordinate set of $k = 1,...,K$ for each layer. The multiplicative inverse gamma prior[21] of shrinkage parameters is $\tau_r^{-1} = \prod_{u=1}^{r} \delta_u^{-1}$, r=1,...,R , $\delta_1 \sim Gamma(a_1, 1)$, $\delta_{u>1} \sim Gamma(a_2, 1)$, $\left(\tau_h^k\right)^{-1} = \prod_{v=1}^{h}\left(\delta_v^k\right)^{-1}$, h=1,...,H, k=1,...,K , $\delta_1^k \sim Gamma(a_1, 1)$, $\delta_{v>1}^k \sim Gamma(a_2, 1)$.

And consider that the prior of dynamic coefficient is: $\beta_m(t) \sim GP(0, c_m)$, $m = 1,...,M$, where, c_m is the square exponential correlation function $c_m\left(t_i, t_j\right) = \exp\left\{-k_m\left(t_i - t_j\right)^2\right\}$, $k_m > 0$.

Consider the a priori of shared and layer-specific potential coordinates on a finite-time grid $t_1,...,t_n$ as follows.

$$\left\{\bar{x}_{ir}\left(t_1\right),...,\bar{x}_{ir}\left(t_n\right)\right\}^{\mathrm{T}} \sim N_n\left(0, \tau_r^{-1}\Sigma_{\bar{x}}\right) \tag{8}$$

$$\left\{x_{ih}^k\left(t_1\right),...,x_{ih}^k\left(t_n\right)\right\}^{\mathrm{T}} \sim N_n\left(0, \tau_h^{k-1}\Sigma_x\right) \tag{9}$$

independently for $i = 1,...,V$, r=1,...,R, h $= 1,...,H$, $k = 1,...,K$. In equations (8) and (9), the $n \times n$ variance and covariance matrices $\Sigma_{\bar{x}[ij]}$ and $\Sigma_{x[ij]}$ have elements $\Sigma_{\bar{x}[ij]} = \exp\left\{-k_{\bar{x}}\left(t_i - t_j\right)^2\right\}$ and $\Sigma_{x[ij]} = \exp\left\{-k_x\left(t_i - t_j\right)^2\right\}$, which also apply to the baseline process of $\left\{\mu(t_1),...,\mu(t_n)\right\}^{\mathrm{T}} \sim N_n\left(0, \Sigma_\mu\right)$.

3.2. Posterior distribution

Based on the above a priori settings, the posterior distribution of the model parameters is represented as follows.

parameter to be estimated	posterior
η	$Dirichlet\left(\alpha_1 + n_1,...,\alpha_B + n_B\right)$
$\omega_{pq}^k(t)$	$PG(b,c), \quad b < 100$ $N\left(\frac{b}{2c}\alpha, \frac{b\left(\alpha^2 - 1\right)}{4c^2} + \frac{b\alpha}{2c^3}\right), \quad b \geq 100$
μ	$N_n\left(\mu_\mu, \Sigma_\mu\right)$
$\bar{x}_p$	$N_{n \times R}\left(\mu_{\bar{x}_p}, \Sigma_{\bar{x}_p}\right)$
x_p^k	$N_{T \times H}\left(\mu_{x_p^k}, \Sigma_{x_p^k}\right)$
δ_1	$Gamma\left(a_1 + \frac{B \times T \times R}{2}, 1 + 0.5\sum_{l=1}^{R}\theta_l^{(-1)}\sum_{p=1}^{B}\bar{x}_{pm}^{\mathrm{T}}K_{\bar{x}}^{-1}\bar{x}_{pm}\right)$

$\delta_{r\geq 2}$	$Gamma\left(a_2+\frac{B\times T\times(R-r+1)}{2},1+0.5\sum_{l=r}^{R}\theta_l^{(-r)}\sum_{p=1}^{B}\bar{x}_{pm}^{\mathrm{T}}K_{\bar{x}}^{-1}\bar{x}_{pm}\right)$
δ_1^k	$Gamma\left(a_1+\frac{B\times T\times H}{2},1+0.5\sum_{s=1}^{H}\theta_s^{(-1)}\sum_{p=1}^{B}x_{ps}^{k\mathrm{T}}K_x^{-1}x_{ps}\right)$
$\delta_{h\geq 2}^k$	$Gamma\left(a_2+\frac{B\times T\times(H-h+1)}{2},1+0.5\sum_{s=r}^{H}\theta_s^{(-h)}\sum_{p=1}^{B}x_{ps}^{k\mathrm{T}}K_{\bar{x}}^{-1}x_{ps}^{k}\right)$
μ_p^k	$N_n\left(\mu_{\mu_p},\Sigma_{\mu_p}\right)$
β_m	$N_n\left(\Sigma_{\beta_m}\begin{bmatrix}\sum_{i=2}^{V}\sum_{j=1}^{i-1}g_{ijm,t_1}\left(y_{ij,t_1}-1/2-\omega_{ij,t_1}v_{ijm,t_1}\right)\\ \vdots \\ \sum_{i=2}^{V}\sum_{j=1}^{i-1}g_{ijm,t_n}\left(y_{ij,t_n}-1/2-\omega_{ij,t_n}v_{ijm,t_n}\right)\end{bmatrix},\Sigma_{\beta_m}\right)$
γ_{ip}	$\eta_p\prod_{t=t_1}^{t_n}\prod_{k=1}^{K}\prod_{q=1}^{B}\left[\pi_{pq}^k(t)\right]^{\sum_{j\neq i,\tilde{z}_j=q}Y_{ij}^k(t)}\left[1-\pi_{pq}^k(t)\right]^{\sum_{j\neq i,\tilde{z}_j=q}1-Y_{ij}^k(t)}$
z_i	$Categorical(\gamma_i)$

The posterior computation utilizes P′olya-gamma data augmentation for Bayesian logistic regression, which allows for simple and easy-to-handle Gibbs samplers of the conjugate full conditionals. In this paper, the Gibbs sampler algorithm is utilized to sample the joint posterior of all model parameters with the following main steps.

- Calculate the number of clusters given the current assignment z.
- Sample the corresponding P′ olya-gamma enhanced data $\omega_{pq}^k(t)$.
- Update inter-block dynamic averages. Update $\mu(t)=[\mu(t_1),\ldots,\mu(t_n)]^{\mathrm{T}}$ from its fully conditional multivariate Gaussian distribution process.
- Update cross-layer block coordinates. Sample the coordinate vector $\bar{x}_p(t_1),\ldots,\bar{x}_p(t_n)$ for each block and layer.
- Update the intra-layer coordinates. Sample the coordinate vector $x_p^k(t_1),\ldots,x_p^k(t_n)$ for each block and layer.
- Update the covariate coefficients β_m according to the posterior distribution.
- The update of the gamma parameter characterizing the prior in equations $\tau_r^{-1}=\prod_{u=1}^{r}\delta_u^{-1}$ and $\left(\tau_h^k\right)^{-1}=\prod_{v=1}^{h}\left(\delta_v^k\right)^{-1}$ follows conjugate analysis, proving the gamma full conditions.
- Updates the dynamic average within the block. Sample the vector $\mu_p^k(t)=\left[\mu_p^k(t_1),\ldots,\mu_p^k(t_n)\right]^{\mathrm{T}}$ for each block and layer.
- Dynamic multilayer block probabilities are updated by applying equation (3) to samples of the baseline process, cross-layer coordinates, and intra-layer coordinates.
- Update the block allocation. Sample potential block allocations z in order and indicate z_i^* if the allocation of node i has been updated and z_i otherwise.

Repeat the above steps until the algorithm converges.

4. Experimental data and result analysis

4.1. Data sets and network description

In order to evaluate the effectiveness and adaptability of this method, this paper selects a set of real business relationship data sets (https://data.world/datasyndrome/relatobusiness-graph-database) collected by Relato. Based on these data, a large business relationship network structure diagram is created as shown in Figure 1. The pairs of relationships include 'partners', 'customers', 'competitors', and 'investments'. The dataset is processed into a K=4-layer network. Finally, 151 companies were selected as nodes, and retained the 5 largest industries, such as 'health care' and 'finance', as node covariates, resulting in a multi-layer network of 151*151*4, and considered a time step of T = 6. This paper aims to combine the node covariates to examine the dynamic evolution of the business relationship network structure, the pairwise relationship between companies over time, and the detection of corporate communities.

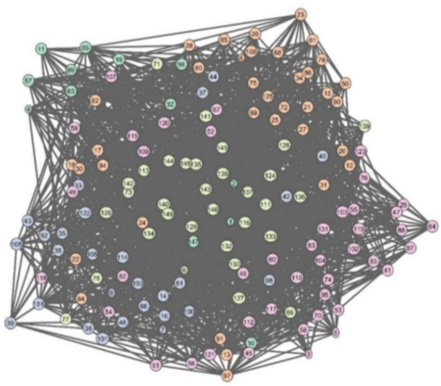

Figure 1. Business relationship network structure diagram.

The above diagram shows the business relationship network structure of 151 companies. The 5 colors in the diagram represent the 5 different industries to which the company belongs. And the more connections exist the larger the node of the company is, and vice versa the smaller it is.

4.2 Experimental results and analysis

4.2.1 Construction of dynamic multi-layer block network

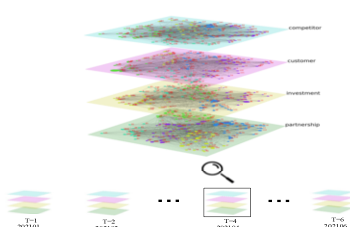

Figure 2. Multi-layer block business relationship network at time t=1,..., 6.

In the constructed dynamic multi-layer block network, the node covariate industry will be regarded as its community label. Figure 2 shows the multi-layer network structure diagram in June 2021. In the first layer of competitor network layer, if there is a competitor relationship between the two companies, there is a connection between them, and it is clear that companies in the same industry often have a competitor relationship, because companies of the same color are mostly close to each other, and only a very small number of companies are in an abnormal position. And with the evolution of time, the multi-layer network structure is also constantly changing, indicating that the pairwise relationship between companies will change within a certain period of time. The relevant network statistics are shown in Table 1.

Table 1. Statistical characteristics of business relationship network

layer	node	edge	network density	average shortest path length	average degree	diameter connection	efficiency	connectivity
1- competitor	312	1519	0.134	1.951	20.119	1	0.433	0.877
2- customer	312	1508	0.133	1.963	19.987	1	0.312	0.878
3- investment	312	1501	0.133	1.986	19.881	1	0.416	0.879
4- partnership	312	1911	0.151	1.801	45.311	1	0.447	0.853

The dynamic multi-layer block network model is further fitted to a selected subset of the complete multi-layer graph shown in Figure 2, including 151 companies in the competitor layer and the investment layer (K=2) network. At the same time, the time step is still considered as T=6 to estimate its potential coordinates.

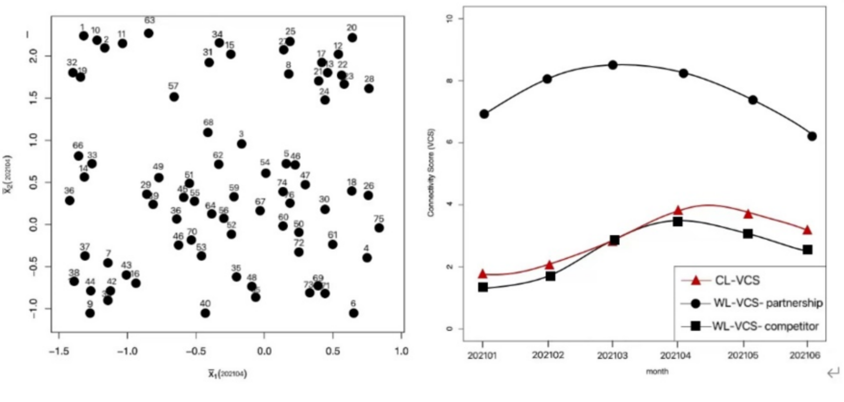

Figure 3. Estimated cross-layer coordinates for all companies for April 2021.

Figure 3 (left) shows the cross-layer coordinates of all companies in April 2021. It can be seen from the diagram that there is a clear cluster structure, indicating that the analysis of adding block structure can better explain its network structure. From Figure 3 (right), we can see the dynamic evolution of the cross-layer and intra-layer vertex connectivity scores of all companies. It can be clearly seen that the intra-layer scores of competitors are growing steadily, while the scores of the partner layer are still high, but the downward trend is obvious.

4.2.2 Dynamic multi-layer prediction of business relationship network

This paper uses available industry company data to verify the proposed extended model by fitting and predicting a large dynamic multi-layer graph. From the aspects of classification accuracy and estimation time, the dynamic multi-layer network model and the dynamic multi-layer block network model are compared, and whether the block structure of the dynamic multi-layer block network model can implement meaningful corporate community detection is studied.

Firstly, the performance of the dynamic multi-layer network model and the dynamic multi-layer block network model is compared. The first 5 months of the sample are used to train the model, that is $t=\{t_1,\ldots,t_5\}$, and the data of the last 1 month are used for out-of-sample prediction. Figure 4 (left) shows the ROC curve of the two-model test data with $B=\{3,4,5\}$ blocks.

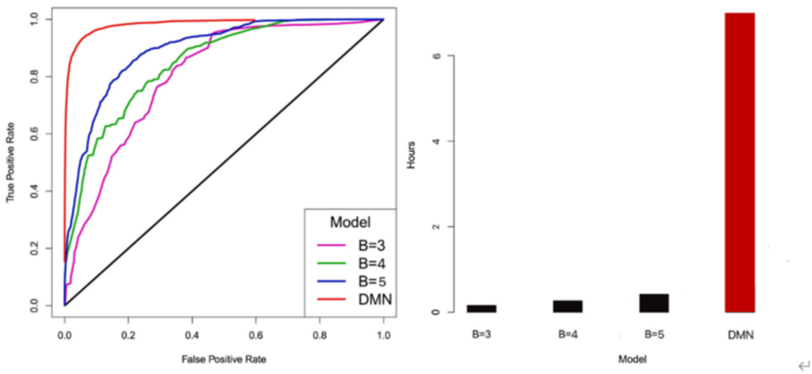

Figure 4. ROC curves for different block numbers (left) and the model estimation time (right).

It can be seen from the above diagram that the dynamic multi-layer network model is a very accurate classifier, but because it is estimated to be N(N-1)/2KT, the dynamic multi-layer block network model is estimated to be B(B+1)/2KT, so the latter calculation cost is much lower than the former. It can be clearly seen from the right of Figure 4 that the performance of the dynamic multi-layer block network model increases with the increase of the number of blocks, and the time spent on estimation is significantly reduced. At the same time, Figure 5 shows the dynamic multi-layer block network model of B = 5 block and the ROC curve of the dynamic multi-layer model. It can be seen from the figure that the worst-structured partner network is the most difficult to predict.

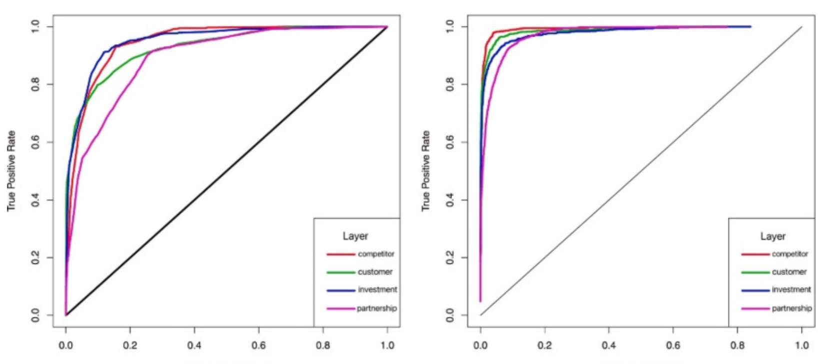

Figure 5. Layer-wise ROC curves from the proposed model with B = 5 (left) and the DMN (right).

The five firm industry clusters tested by the dynamic multilayer block model are also given. The fourth cluster is the largest, including 43 companies, such as Clearswift, Symantec, Imperva, etc., among which there are several abnormal node companies : Trace3 (1), Riverbed, Nokia, Trend Micro (2), VMWare (3), Assessment Systems (5) ; the first cluster is the smallest, including only 13 companies, including Safend, Institute of Asset Management (4) ; the node companies included in clusters 2,3, and 5 are shown in the above table. These three clusters also have several abnormal nodes, such as Software, FireMon, Dell, AT&T, and Hewlett Packard.

Finally, this paper compares the prediction performance of the proposed method with several popular non-probabilistic algorithms such as Katz Index (Katz), Restarted Random Walk (RWR) based on PageRank algorithm.

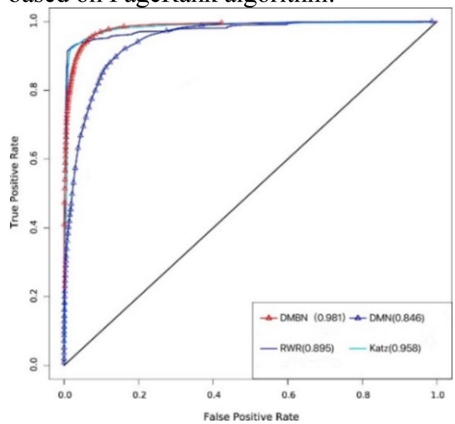

Figure 6. ROC curves for probabilistic and similarity-based prediction methods.

Figure 6 illustrates the ROC curves as well as the area under the curve (AUC) for DMN, DMBN, etc. with 5 blocks, from which it can be seen that DMBN and Katz index are the best probabilistic and similarity-based classifiers, respectively.

5. Conclusion

In this paper, we propose a covariate-assisted dynamic multilayer block network model that models the edge probabilities between nodes by means of a latent Gaussian process to obtain a flexible time series analysis. It not only demonstrates the dynamic evolution process of the multilayer network, i.e., the pairwise relationship between the firms changes in a certain period of time, but also allows time-series clustering of the connection dynamics of the network nodes and related community detection. It also has a relatively low estimation time cost and is better able to capture the dynamic, multilayer, and other properties of large networks than other models. Secondly, the node covariates are incorporated into the multi-layer dynamic network to obtain better community detection accuracy. Experiments show that the model has wide applicability and is more suitable for large-scale social network analysis. In addition, in terms of model comparison, the out-of-sample prediction performance of the dynamic multi-layer block network model is much better than that of the dynamic multi-layer network model, and the computational cost of the former is much lower than that of the latter. The estimation time for the dynamic multilayer block network model ranged from 25 minutes (B=3) to 1.2 hours (B=5), while the dynamic multilayer network model took more than 6 hours.

References

[1] Brandes U, Robins G, McCranie A, et al. What is network science?. Network science, 2013, 1(1): 1-15.
[2] Frantz T L. Garry Robins: Doing social network research: network-based research design for social scientists. SAGE Publications. 2017: 587-589.
[3] Yasami Y. A new knowledge-based link recommendation approach using a non-parametric multilayer model of dynamic complex networks. Knowledge-Based Systems. 2018, 143: 81-92.
[4] Leetaru K, Schrodt P A. Gdelt: Global data on events, location, and tone, 1979–2012. ISA annual convention; 2013 April 3-6; San Francisco, California: 2013, 2(4): 1-49.
[5] Blondel V D, Decuyper A, Krings G. A survey of results on mobile phone datasets analysis. EPJ data science. 2015, 4: 1-55.
[6] Shang Y. Characterization of expansion-related properties of modular graphs. Discrete Applied Mathematics. 2023, 338: 135-144.
[7] Shang Y. Resilient consensus for robust multiplex networks with asymmetric confidence intervals. IEEE Transactions on Network Science and Engineering. 2020, 8(1): 65-74.
[8] Hoff P D, Raftery A E, Handcock M S. Latent space approaches to social network analysis. Journal of the american Statistical association, 2002, 97(460): 1090-1098.
[9] Gollini I, Murphy T B. Joint modeling of multiple network views. Journal of Computational and Graphical Statistics, 2016, 25(1): 246-265.
[10] DAngelo, S., Murphy, T. B., Alf`o, M., et al. Latent space modelling of multidimensional networks with application to the exchange of votes in eurovision song contest. The Annals of Applied Statistics, 2019, 13(2): 900‑930.
[11] Durante D, Dunson D B. Bayesian dynamic financial networks with time-varying predictors. Statistics & Probability Letters, 2014, 93: 19-26.
[12] Durante D, Dunson D B. Nonparametric Bayes dynamic modelling of relational data. Biometrika, 2014, 101(4): 883-898.
[13] Durante, Daniele, and David B. Dunson. "Locally adaptive dynamic networks." 2016: 2203-2232.
[14] Durante D, Mukherjee N, Steorts R C. Bayesian learning of dynamic multilayer networks. Journal of Machine Learning Research, 2017, 18(43): 1-29.
[15] Carmona C U, Martinez-Jaramillo S. Learning of weighted multi-layer networks via dynamic social spaces, with application to financial interbank transactions, Complex Networks and Their Applications VIII: Volume 2 Proceedings of the Eighth International Conference on Complex Networks and Their Applications COMPLEX NETWORKS 2019 8. Springer International Publishing, 2020: 722-735.
[16] Yildirimoglu M, Kim J. Identification of communities in urban mobility networks using multi-layer graphs of network traffic. Transportation Research Part C: Emerging Technologies. 2018, 89: 254-267.
[17] Yap M, Luo D, Cats O, et al. Where shall we sync? Clustering passenger flows to identify urban public transport hubs and their key synchronization priorities. Transportation Research Part C: Emerging Technologies. 2019, 98: 433-448.
[18] Tian Z, Zhou J, Szeto W Y, et al. The rebalancing of bike-sharing system under flow-type task window. Transportation research part C: emerging technologies. 2020, 112: 1-27.
[19] Rodriguez-Deniz H, Villani M, Voltes-Dorta A. A multilayered block network model to forecast large dynamic transportation graphs: An application to US air transport. Transportation Research Part C: Emerging Technologies, 2022, 137: 103556.
[20] Snijders T A B, Lomi A, Torló V J. A model for the multiplex dynamics of two-mode and one-mode networks, with an application to employment preference, friendship, and advice. Social networks, 2013, 35(2): 265-276.
[21] Bhattacharya A, Dunson D B. Sparse Bayesian infinite factor models. Biometrika, 2011, 98(2): 291-306.